Interaction Notes

Note 213

September 1974

Penetration of Electromagnetic Fields Through Small Apertures in Planar Screens: Selected Data

Donald R. Wilton
Chalmers M. Butler
K. R. Umashankar
University of Mississippi
University, Mississippi 38677

Abstract

Selected numerical data are presented for penetration of electromagnetic waves through apertures in planar screens. Major attention is focused upon electrically small, rectangular apertures, and, for a specified length-to-width ratio, five numbers are given which enable one to compute equivalent electric and magnetic dipole moments due to an incident plane wave of any polarization, angle of incidence, and magnitude. Convergence of solutions is discussed as is the accuracy of equivalent dipole representations of fields which penetrate an aperture.

This study was performed under subcontract to

The Dikewood Corporation
1009 Bradbury Drive, S.E.
University Research Park
Albuquerque, New Mexico 87106

and has been fully supported by the Defense Nuclear Agency (DNA) under

DNA Subtask EB088
EMP Interaction and Coupling
DNA Work Units 32 and 33
Coupling Characteristics of Apertures
Coaxial Cables

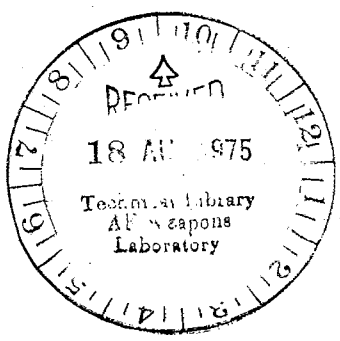

CONTENTS

ILLUSTRATIONS

ILLUSTRATIONS (continued)

SECTION I

INTRODUCTION

The classic problem of penetration of time-harmonic electromagnetic energy through an aperture in an infinite conducting screen is of immense practical importance and has been studied for many years, yet there is not available a comprehensive set of data describing the electromagnetic fields in and near apertures of various shapes and sizes.

The purpose of the research reported here is to present data characterizing aperture diffraction for large and small rectangular and circular apertures with primary emphasis upon small rectangular shapes. Results have been obtained for elliptic and diamond-shaped apertures, and the numerical solution procedure can be used for apertures of general shape if desired. The general problem of interest is depicted in Figure 1, where one sees an arbitrarily shaped aperture A in a perfectly conducting planar screen of infinite extent, located in the x-y plane and residing in a homogeneous medium characterized by $(\mu,\varepsilon,\sigma=0)$. The aperture/screen is illuminated by a uniform plane electromagnetic wave having an electric field

$$\bar{E}^i = \bar{e}^i \, e^{-jk(x\cos\alpha + y\cos\beta + z\cos\gamma)} \tag{1}$$

where k is 2π/wavelength, where

$$\bar{e}^i = e_x^i \hat{u}_x + e_y^i \hat{u}_y + e_z^i \hat{u}_z \tag{2}$$

is the constant complex vector representing the magnitude and phase of $\bar{E}^i$ at (0,0,0), and where the direction cosines in (1) are defined relative to the direction of propagation $\hat{u}$:

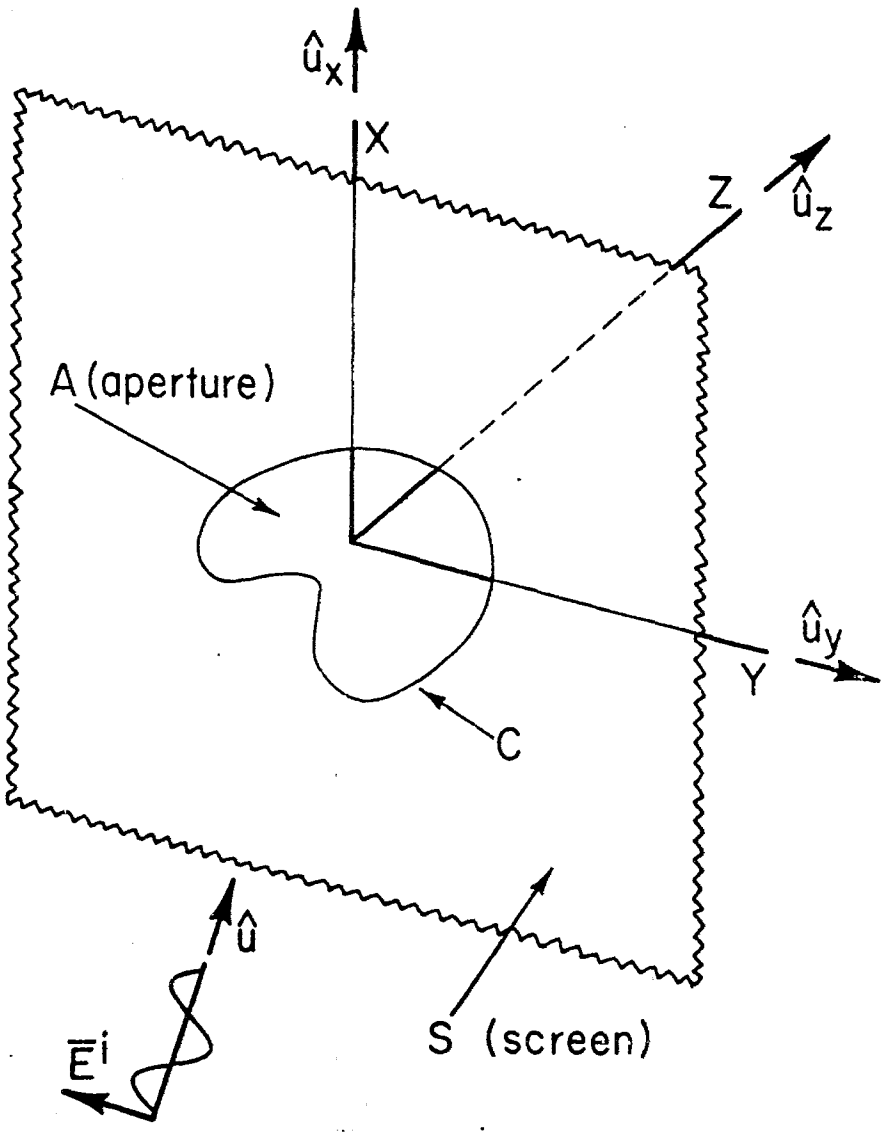

Figure 1. Aperture in Conducting Screen Illuminated by Incident Field

$$\cos\alpha = \hat{u} \cdot \hat{u}_x \quad , \tag{3a}$$

$$\cos\beta = \hat{u} \cdot \hat{u}_y \quad , \tag{3b}$$

$$\cos\gamma = \hat{u} \cdot \hat{u}_z \quad . \tag{3c}$$

The data presented here are based upon recently developed aperture integral equations [1,2]* and results obtained from their numerical solutions [2,3]. In an earlier report [2], integral equations valid for the full dynamic (time-harmonic) aperture/screen problem are derived and a numerical solution procedure is outlined. In Interaction Note 149 [1], integral equations are developed which are based upon expansions of quantities of interest in power series in reciprocal wavelength. Such an analysis involving a so-called Rayleigh series provides a system of integral equations which completely characterizes the aperture problem at frequencies below the first resonance (in the circle of convergence of the power series) but, due to primary interest in electrically small apertures, only the two sets which yield solutions valid to zeroth and first order in reciprocal wavelength are solved numerically in [3].

In particular, this report includes a discussion of the Rayleigh series solutions and the equivalent dipole moments for apertures, a discussion of solution convergence and its improvement, and a comparison of the fields which penetrate an aperture calculated from equivalent dipole moments and from the exact aperture field distribution. Dipole moments for small rectangular apertures are given and are tabulated in a manner which provides a complete characterization of the associated aperture fields for a plane wave incident field having any polarization

*Numbers in [ ] refer to entries under REFERENCES.

and angle of incidence.

Also, results obtained from solutions of the full dynamic aperture equations [2] are included showing dipole moments for the circular aperture as well as magnetic current distributions for a large square aperture. In addition, Rayleigh series and dynamic results are compared for several rectangular apertures.

SECTION II

THE RAYLEIGH SERIES ANALYSIS AND EQUIVALENT PROBLEM PARTITIONING

The Rayleigh series formulation discussed in a previous note [1] has the advantage that when the frequencies are low enough to allow a two-term approximation the aperture problem may be partitioned into a series of partial problems, the solutions to which permit one to synthesize by superposition the total solution for an arbitrarily illuminated aperture. This partitioning is summarized below.

The frequency of the plane wave illumination is assumed to be low enough that the first two terms in the Rayleigh series for the magnetic current*

$$\bar{M} = \bar{M}_0 + k\bar{M}_1 + \ldots \tag{4}$$

where k is the wavenumber, are sufficient to approximate the magnetic current in the aperture. From the above free space magnetic current distribution $\bar{M}$, one may then determine the aperture electric field according to $\bar{E}^a = \frac{1}{2}\bar{M}\times\hat{u}_z$ where $\bar{E}^a$ here is in the plane of the aperture.

The series coefficients of zeroth and first order magnetic current distributions, $\bar{M}_0$ and $\bar{M}_1$, are the solutions of two pairs of integral equations [1]. These equations are, for $\bar{M}_0$,

$$\nabla_t^2 \iint_A \bar{M}_0(\bar{r}')R^{-1}(\bar{r},\bar{r}')ds' = \bar{0} \quad , \quad \bar{r} \in A \tag{5a}$$

---

*To be consistent with [1], $\bar{M}$ is the illuminated-side, free space equivalent magnetic current (surface) in the aperture.

$$\mathrm{div}_t \iint_A [\bar{M}_0(\bar{r}')\times\hat{u}_z]R^{-1}(\bar{r},\bar{r}')ds' = 4\pi e_z^i \quad , \bar{r} \in A \quad (5b)$$

and, for $\bar{M}_1$,

$$\nabla_t^2 \iint_A \bar{M}_1(\bar{r}')R^{-1}(\bar{r},\bar{r}')ds' = -j4\pi\cos\gamma(\hat{u}_z \times e^{-i}) \quad (6a)$$
$$,\bar{r}\epsilon A$$

$$\mathrm{div}_t \iint_A [\bar{M}_1(\bar{r}')\times\hat{u}_z]R^{-1}(\bar{r},\bar{r}')ds' = -j4\pi e_z^i(\hat{u}\cdot\bar{r})_0 \quad (6b)$$

where

$$R(r,r') = [(x-x')^2 + (y-y')^2]^{\frac{1}{2}}$$

and

$$(\hat{u}\cdot\bar{r})_0 = x\cos\alpha + y\cos\beta.$$

Several observations may be made concerning the solutions of (5) and (6) which simplify the characterization of an aperture of a given shape. For example, as can be shown from a study of Equations (5) and (6), the current distributions $\bar{M}_0(\bar{r})$ and $\bar{M}_1(\bar{r})$ simply become the current distributions $\bar{M}_0(\bar{r}/\Omega)$ and $\Omega\bar{M}_1(\bar{r}/\Omega)$ when some reference linear dimension d of the aperture is expanded or contracted by the factor Ω with the aperture shape fixed. Furthermore, it is noted from Equations (5a) and (5b) that $\bar{M}_0$ is proportional to e_z^i only, independent of the angle of incidence, whereas $\bar{M}_1$ depends in a more complicated fashion on the various components of $\bar{e}^i$ and the angle of incidence. Nevertheless, a partitioning of $\bar{M}_1$ into a set of four linearly independent partial currents can be effected in such a way that the components of $\bar{e}^i$ and

the angle of incidence affect only the magnitude of each partial current. In Table 1 is found the single problem associated with $\bar{M}_0$ and the four partial problems relating to $\bar{M}_1$ are listed in Table 2. The second and third columns of Table 2 give the four linearly independent driving functions for each partial problem and the column sums yield the total driving functions on the right-hand sides of Equations (6a) and (6b). Hence, the total first order current must be given by

$$\bar{M}_1 = \bar{M}_1^{I} + \bar{M}_1^{II} + \bar{M}_1^{III} + \bar{M}_1^{IV} \tag{7}$$

where each superscripted current is a solution to the corresponding case in Table 2. From Tables 1 and 2 and the discussion above, one may define a complete set of linearly independent normalized basis currents which are dimensionless and which characterize a small aperture of a given shape and reference linear dimension d:

$$\bar{m}_0 = \frac{\bar{M}_0}{e_z^i} \tag{8a}$$

$$\bar{m}_1^{I} = \frac{\bar{M}_1^{I}}{d \cos\gamma e_x^i} \tag{8b}$$

$$\bar{m}_1^{II} = \frac{\bar{M}_1^{II}}{d \cos\gamma e_y^i} \tag{8c}$$

$$\bar{m}_1^{III} = \frac{\bar{M}_1^{III}}{d \cos\alpha e_z^i} \tag{8d}$$

$$\bar{m}_1^{IV} = \frac{\bar{M}_1^{IV}}{d \cos\beta e_z^i} \tag{8e}$$

Table 1

Properties of Zeroth Order Magnetic Current for Symmetric Aperture

$v_t^2 \iint_A \bar{M}_o R^{-1} ds'$	$\mathrm{div}_t \iint_A [\bar{M}_o \times \hat{u}_z] R^{-1} ds'$	Symmetry Property of $\bar{M}_o$	Normalized Dipole Moments
0	$4\pi e_z^i$	$M_{o_x}(x,y) = -M_{o_x}(-x,y) = M_{o_x}(x,-y)$	$\bar{p}_{o_e} = \frac{p_{e_z}}{\varepsilon d^3 e_z^i} \hat{u}_z$
		$M_{o_y}(x,y) = M_{o_y}(-x,y) = -M_{o_y}(x,-y)$	$\bar{p}_{o_m} = \bar{0}$

Table 2

Partitioned Excitation and Corresponding Partial First Order Magnetic Current for Symmetric Apertures

Case	$\nabla_t^2 \iint_A \bar{M}_1 R^{-1} ds'$	$\mathrm{div}_t \iint_A [\bar{M}_1 \times \hat{u}_z] R^{-1} ds'$	Symmetry Properties of $\bar{M}_1$	Normalized Dipole Moments
I	$-j4\pi \cos\gamma e_x^i \hat{u}_y$	0	$M_{1_x}^I(x,y) = -M_{1_x}^I(-x,y) = -M_{1_x}^I(x,-y)$	$\bar{p}_{1_m}^I = \frac{\eta p_{m_y}^I}{d^3 \cos\gamma e_x^i} \hat{u}_y$
			$M_{1_y}^I(x,y) = M_{1_y}^I(-x,y) = M_{1_y}^I(-x,y)$	$\bar{p}_{1_e}^I = \bar{0}$
II	$+j4\pi \cos\gamma e_y^i \hat{u}_x$	0	$M_{1_x}^{II}(x,y) = M_{1_x}^{II}(-x,y) = M_{1_x}^{II}(x,-y)$	$\bar{p}_{1_m}^{II} = \frac{\eta p_{m_x}^{II}}{d^3 \cos\gamma e_y^i} \hat{u}_x$
			$M_{1_y}^{II}(x,y) = -M_{1_y}^{II}(-x,y) = -M_{1_y}^{II}(x,-y)$	$\bar{p}_{1_e}^{II} = \bar{0}$
III	0	$-j4\pi e_z^i x \cos\alpha$	$M_{1_x}^{III}(x,y) = -M_{1_x}^{III}(-x,y) = -M_{1_x}^{III}(x,-y)$	$\bar{p}_{1_m}^{III} = \frac{\eta p_{m_y}^{III}}{d^3 \cos\alpha e_z^i} \hat{u}_y$
			$M_{1_y}^{III}(x,y) = M_{1_y}^{III}(-x,y) = M_{1_y}^{III}(x,-y)$	$\bar{p}_{1_e}^{III} = \bar{0}$
IV	0	$-j4\pi e_z^i y \cos\beta$	$M_{1_x}^{IV}(x,y) = M_{1_x}^{IV}(-x,y) = M_{1_x}^{IV}(x,-y)$	$\bar{p}_{1_m}^{IV} = \frac{\eta p_{m_x}^{IV}}{d^3 \cos\beta e_z^i} \hat{u}_x$
			$M_{1_y}^{IV}(x,y) = -M_{1_y}^{IV}(-x,y) = -M_{1_y}^{IV}(x,-y)$	$\bar{p}_{1_e}^{IV} = \bar{0}$

For small apertures, the radiated fields due to the presence of the aperture can be found in terms of equivalent dipole moments of the aperture which radiate into free space. In terms of the magnetic currents, the dipole moments are given by

$$\bar{P}_e = \frac{\varepsilon}{2} \iint_A \bar{M}(\bar{r}') \times \bar{r}' ds' \tag{9}$$

for the electric dipole moment and for the magnetic dipole moment

$$\bar{P}_m = \frac{1}{jk\eta} \iint_A \bar{M}(\bar{r}') ds' \tag{10}$$

where η is the characteristic impedance of the homogeneous medium. The dipole moments (9) and (10) may be used in conjunction with the short circuit fields ($\bar{E}^{sc}$, $\bar{H}^{sc}$) [1] to compute total fields on the illuminated side of the aperture ($z<0$). For fields on the shadow side of the aperture, a negative sign is needed with each equation, (9) and (10), and total fields for $z>0$ may be approximated by the moments above. For aperture shapes which have two perpendicular mirror symmetry planes such as those considered here, e.g., squares, rectangles, circles, and ellipses, $\bar{M}_0$ does not contribute to the magnetic moment and $\bar{M}_1$ does not contribute to the electric moment. This decoupling may easily be seen as a consequence of the various symmetry properties of $\bar{M}_0$ and the basis currents in Equation (7). These symmetries are tabulated in Tables 1 and 2.

The set of dipole moments of the individual basis magnetic currents of the partial problems suggested in Tables 1 and 2 also

forms a set of basis elements for the dipole moments of an aperture. The dependence of the dipole moments on the material medium, aperture size, and incident field may be factored out to yield the normalized dipole moments of the aperture which are given in Tables 1 and 2. To compute the actual dipole moments of an aperture whose characteristic dimension is d, one forms the following linear combinations of the normalized dipole moments:

$$\bar{P}_e = \epsilon d^3 e_z^i \bar{p}_{o_e} \tag{11}$$

and

$$\bar{P}_m = \frac{d^3}{\eta} [\cos\gamma e_x^i \bar{p}_{1_m}^{I} + \cos\gamma e_y^i \bar{p}_{1_m}^{II}$$

$$+ \cos\alpha e_z^i \bar{p}_{1_m}^{III} + \cos\beta e_z^i \bar{p}_{1_m}^{IV}] \quad . \tag{12}$$

Hence, to the approximation that the dipole moments represent the fields radiated by an aperture, the first two terms of the Rayleigh series for the radiated fields can be expressed in terms of five constant vectors which characterize an aperture of any given shape.

SECTION III

SCALED DIPOLE MOMENTS

Because, for the purposes of numerical computation, the aperture is divided into a set of subdomains and the integral equation is enforced at the center of each subdomain, the boundary conditions of a given problem are not generally satisfactorily met in a numerical solution. Such is seen immediately when the fields resulting from the calculated currents are examined near the edges of the aperture. While other choices of basis functions for the magnetic current representation tend to alleviate this difficulty, they become awkward and/or expensive to handle in the two-dimensional integral equations considered here. The boundary condition is numerically enforced at all the match points, however, and the interpolating fields between the match points usually approximate the boundary condition in some average sense. As a result, the aperture currents calculated usually correspond to those of an aperture slightly smaller by approximately a full subdomain (one-half subdomain at each edge) along each linear dimension. This phenomenon only slightly affects the convergence of the magnetic current since $\overline{M}_0$ is independent of d and $\overline{M}_1$ depends only linearly on d. However, in the calculation of dipole moments, additional complications arise. These are associated with the edge behavior of the current, viz., the current normal to an edge must vanish and the current parallel to an edge becomes singular. Usually the condition on the normal current is enforced numerically by requiring the current in the edge subdomain to be zero. Interpolating the current through

the center of the subdomains results in an aperture which, for the normal component of current, is short by one-half of a subdomain at each edge. Consequently, integration over the component of magnetic current normal to an aperture edge in calculation of dipole moments, Equations (9) and (10), covers an aperture having a reduced width which is one subdomain smaller than the actual width. In the case of current parallel to an edge, the calculated current in the moment method tends to have a slightly lower average than the actual average current in the subdomain which a pulse basis set attempts to represent. Hence, when dipole moments are numerically calculated, the edge (parallel) current contribution is too small. This effect may be thought of as modeling an aperture which is slightly smaller than the correct aperture. If one assumes for simplicity that the effective aperture size is reduced by one subdomain, then all the effects above result in an effective aperture whose area is smaller by approximately half the total area of the edge subdomains. Since dipole moments vary as d^3 for an aperture of a given shape and reference dimension d (Tables (1) and (2)), the dipole moments are extremely sensitive to changes in effective aperture size. As a result, convergence of the computed dipole moments is very slow as seen in Figures 2 and 3 where the magnetic dipole moments for a normally illuminated square and circular aperture are given, respectively, as a function of the reciprocal of the number of subdomains along a given dimension.

Since, from the discussion above, the length dependence of the moments and the effective length of solutions from the numerical calculations are known a priori, a scaling factor can be introduced,

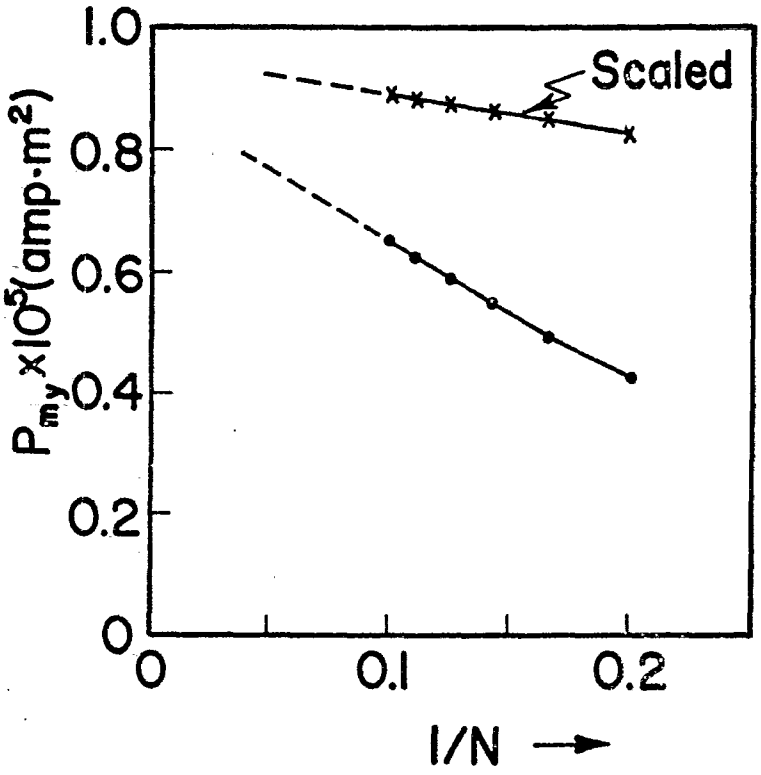

Figure 2. Convergence of Illuminated-Side P_{m_y} (Free Space) for Square Aperture ($a = b = 0.15\lambda$, $\bar{e}^i = 1\ \hat{u}_y$ Volt/Meter, Normal Incidence)

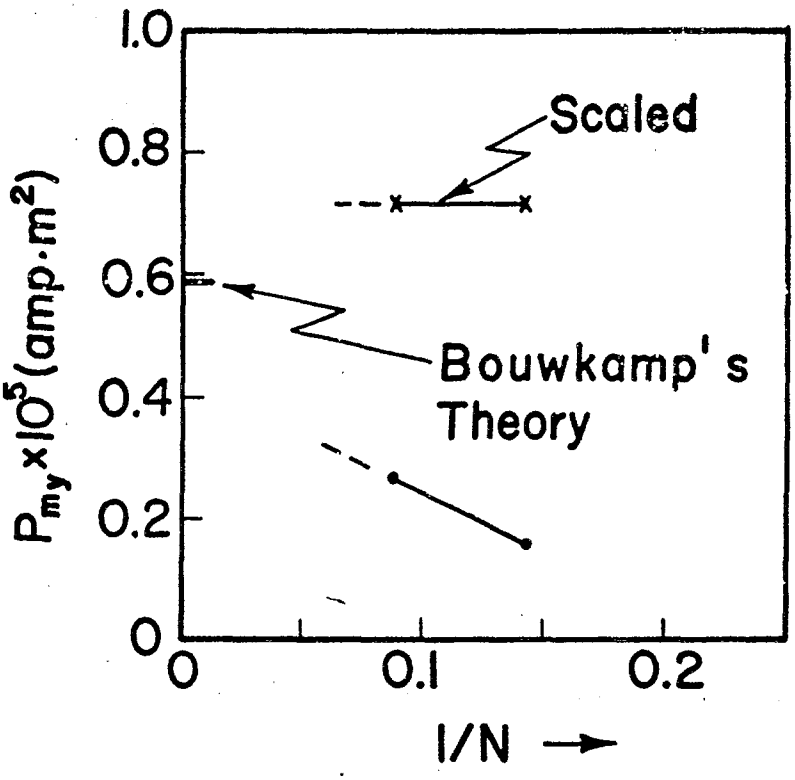

Figure 3. Convergence of Illuminated-Side P_{m_y} (Free Space) for Circular Aperture (Diameter = 0.15λ, $\bar{e}^i = 1\,\hat{u}_y$ Volt/Meter, Normal Incidence)

$$\kappa = \left[\frac{A}{A_{eff}}\right]^{\frac{3}{2}} \tag{13}$$

which can be used to scale the data to a proper size aperture. In (13), A is the actual area of the aperture and A_{eff} is the effective area obtained by deleting half the area of the edge subdomains. Note that in the case of a circle, for instance, there is a significant portion of the area uncovered by the rectangular subdomains, since they have been chosen interior to the bounding contour [2]. Equation (13) also takes this effect into account. Further note that, if the effective aperture has the same shape as the given aperture, the scaling factor reduces to the correct dependence on the aperture length. However, if subdomains have different heights than widths, the scaling factor effectively employs a geometric average length to achieve the scaling, thus preserving the dependence of linear dimension in any direction but ignoring the change in dipole moment due to the change in effective shape. The improved convergence of the scaled dipole moment for the square aperture is noted in Figure 2, where the scaling factor becomes approximately

$$\kappa = \left[\frac{MN}{(M-1)(N-1)}\right]^{\frac{3}{2}} \tag{14}$$

with M=N.

In (14) above, M and N are the numbers of subdomains along the x and y directions, respectively, of the aperture.

The improvement in the dipole moment convergence is even more dramatic when the scaling factor is used with the dipole moments of

a circular aperture, Figure 3, where the subdomains do not completely fill the aperture. Here, the scaling factor is

$$\kappa = \left[\frac{\pi a^2}{(M-J/2)\Delta x\Delta y}\right]^{\frac{3}{2}} \tag{15}$$

where M and J are the number of interior and boundary subdomains, respectively, and $\Delta x\Delta y$ is the area of a subdomain.

In Table 3 the scaled and unscaled dipole moments of rectangular apertures of height to width ratios of a/b = 1,2,3,10, and 20 are tabulated. It is particularly noted that the scaled dipole moments of a square aperture are approximately one and one-half times those of a circular aperture of radius a. Also note that $|\bar{p}_{1_m}^{I}| \doteq |\bar{p}_{1_m}^{III}|$ and $|\bar{p}_{1_m}^{II}| \doteq |\bar{p}_{1_m}^{IV}|$. Using the reciprocity theorem, one can show theoretically that these approximations observed from the numerical results should be exact. Finally, one calls attention to the utility of Table 3, the data of which enables one to determine readily the dipole moments for small rectangles subject to a uniform plane wave incident field of any polarization, angle of incidence, and magnitude.

Table 3

Normalized Dipole Moments (Illuminated Side, Free Space) of a Rectangular Aperture of Height 2a and Width 2b (d=a)

NORMALIZED DIPOLE MOMENTS	COMPUTED MOMENTS	SCALED MOMENTS	COMPUTED MOMENTS	SCALED MOMENTS	COMPUTED MOMENTS	SCALED MOMENTS	COMPUTED MOMENTS	SCALED MOMENTS	COMPUTED MOMENTS	SCALED MOMENTS
	a/b=1		a/b=2		a/b=3		a/b=10		a/b=20	
$\bar{p}_{o_e} \cdot \hat{u}_z$	-3.235	-4.438	-1.024	-1.455	-0.4590	-0.7025	-0.0347	-0.0675	-0.0103	-0.0200
$\bar{p}_{1_m}^{I} \cdot \hat{u}_y$	6.270	8.600	1.338	1.901	0.4826	0.7386	0.0249	0.0484	0.0074	0.0144
$\bar{p}_{1_m}^{II} \cdot \hat{u}_x$	-6.270	-8.600	-4.131	-5.869	-3.245	-4.966	-1.710	-3.323	-1.369	-2.467
$\bar{p}_{1_m}^{III} \cdot \hat{u}_y$	-6.388	-8.763	-1.390	-1.975	-0.5054	-0.7736	-0.0287	-0.0558	-0.0105	-0.0204
$\bar{p}_{1_m}^{IV} \cdot \hat{u}_x$	6.388	8.763	4.022	5.714	3.141	4.807	1.600	3.111	1.122	2.181

SECTION IV

CALCULATION OF FIELDS NEAR APERTURE

Often in numerous practical situations, one wishes to calculate the fields which penetrate an aperture as well as those which are scattered back. In the shadow half-space, the total fields can be calculated from knowledge of $\bar{M}$ alone; whereas, in the illuminated half-space, one must add the short-circuit fields to those produced by $\bar{M}$ [1]. For an electrically small aperture one may approximate the aperture-produced fields by making use of the dipole moments calculated for the given aperture. How good the dipole moment approximation to the actual fields is depends upon the electrical size of the aperture, the distance from the aperture to the point at which the field is evaluated, and the choice of the coordinate origin with respect to which the dipole moments are calculated. Therefore, since one wishes to take advantage of the simplicity afforded by use of dipole moments to characterize the electromagnetic behavior of an aperture, it is of interest to determine fields directly from the numerically calculated magnetic current $\bar{M}$ as well as from the moments and then to compare values so obtained. Such comparisons enable one to assess the accuracy of fields calculated from moments.

Electric Field from Magnetic Current

The aperture-produced electric field $\bar{E}^a$ may be calculated at a general point $\bar{r}$ from the magnetic current $\bar{M}$ by means of [1]

$$\bar{E}^a(\bar{r}) = \pm \frac{1}{\varepsilon} \operatorname{curl} \bar{F}(\bar{r}) \tag{16}$$

where

$$\bar{F}(\bar{r}) = \frac{\epsilon}{4\pi} \iint_A \bar{M}(\bar{r}') \frac{e^{-jk|\bar{r}-\bar{r}'|}}{|\bar{r}-\bar{r}'|} \, ds' \tag{17}$$

and where $\bar{r}'$ locates the source point in the aperture A. The + sign holds for $z>0$ and the - sign for $z<0$, and $\bar{M}$ is the illuminated-side equivalent magnetic current in the absence of the screen. Knowing $\bar{M}$ from the numerical solution [1, 2, 3] for a given aperture, one may readily perform the operations indicated in (16) and (17) to obtain $\bar{E}^a$. On the shadow side, $\bar{E}^a$ is the total electric field but on the illuminated side the total electric field is $\bar{E}^{sc} + \bar{E}^a$ [1].

Electric Field from Dipole Moments

From knowledge of an equivalent aperture magnetic current distribution $\bar{M}$ in free space, one can determine $\bar{P}_e$ and $\bar{P}_m$ from (9) and (10). $\bar{P}_e$ is always normal to the aperture so one may readily show that the component contributions to $\bar{E}^a$ from the equivalent electric dipole moment are, in the spherical coordinate system of Figure 4,

$$E_r^{ae} = \frac{P_e}{2\pi\epsilon} \frac{e^{-jkr}}{r} \left(j\frac{k}{r} + \frac{1}{r^2}\right) \cos\theta \tag{18}$$

and

$$E_\theta^{ae} = \frac{P_e}{4\pi\epsilon} \frac{e^{-jkr}}{r} \left(j\frac{k}{r} + \frac{1}{r^2} - k^2\right) \sin\theta \quad . \tag{19}$$

$\bar{P}_m$ is always in the plane of the aperture/screen and, in a coordinate system with polar axis along $\bar{P}_m$, the total electric field contributed from this equivalent magnetic dipole is

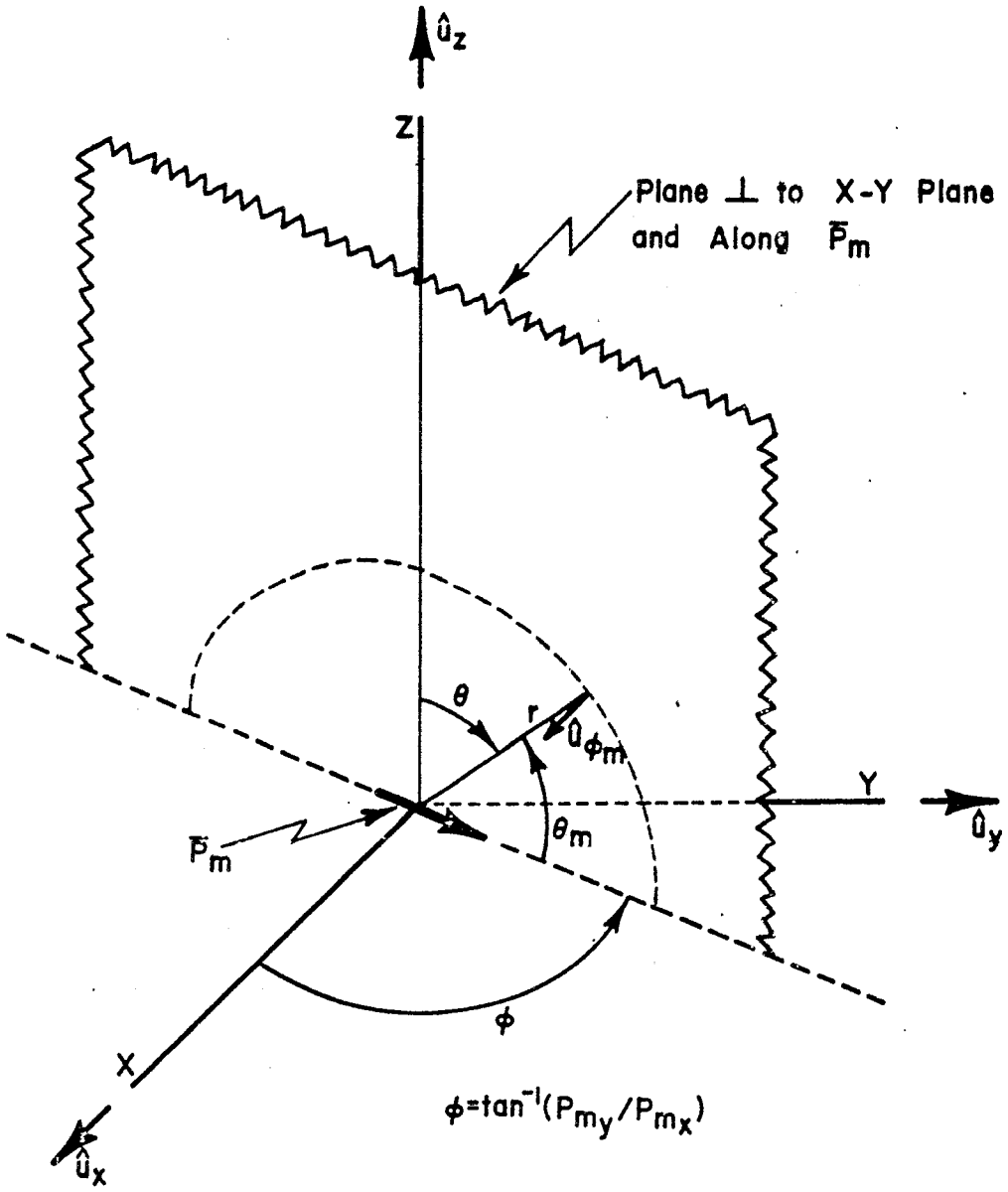

Figure 4. Coordinate System for Dipole Moments

$$\bar{E}^{am} = -\frac{\eta}{4\pi} P_m \frac{e^{-jkr}}{r} \left(j\frac{k}{r} - k^2\right) \sin\theta_m \hat{u}_{\phi_m} \qquad (20)$$

where $\hat{u}_{\phi_m}$ implies that $\bar{E}^{am}$ is ϕ-directed (right hand system) in the coordinate system about the pole along $\bar{P}_m$ and where θ_m is the polar angle.

The nature of this electric field is better understood from reference to Figure 4. In the plane identified there, $\bar{E}^{am}$ can be readily written

$$\bar{E}^{am} = \frac{\eta}{4\pi} (\hat{u}_z \times \bar{P}_m) \frac{e^{-jkr}}{r} \left(j\frac{k}{r} - k^2\right) \cos\theta \quad . \qquad (21)$$

Making use of (18), (19), and (21) one may readily calculate the electric field in the plane specified in Figure 4 and assess the accuracy of the dipole moment approximations.

Figure 5 depicts a rectangular aperture in an infinite screen; reference is made to the symbols defined there in subsequent discussion.

Figure 6 shows the electric field penetrating a square aperture ($2a=2b=0.15\lambda$) subject to normally incident illumination with $e_y^i = 1$ volt/meter and $e_x^i = 0$. In this case $\bar{P}_e = \bar{0}$ so the total field is approximately that of a magnetic dipole of moment $\bar{P}_m$. These approximate values of fields together with exact values from (16) and (17) are both displayed for comparison in Figure 6. One sees good agreement at a radial distance $r = 10a$ but sees significant differences at $3a$ and $2a$. In Figure 7 is displayed the fields penetrating the same aperture subject to edge-on incident illumination with $e_z^i = 1$ volt/meter. The data in this figure is valid for either ($\alpha=0^o$, $\beta=90^o$) or ($\alpha=90^o$, $\beta=0^o$),

and one notes from the symmetry properties of $\overline{M}_1$ in Table 2, Case III and Case IV, and the definition of the magnetic dipole moment (10), that $\overline{P}_m$ is zero for the square aperture with edge-on incidence and, hence, that the field of the equivalent electric dipole approximates the total field. In Figure 7 it is observed that the dipole approximation is somewhat poor near the aperture for edge-on incidence.

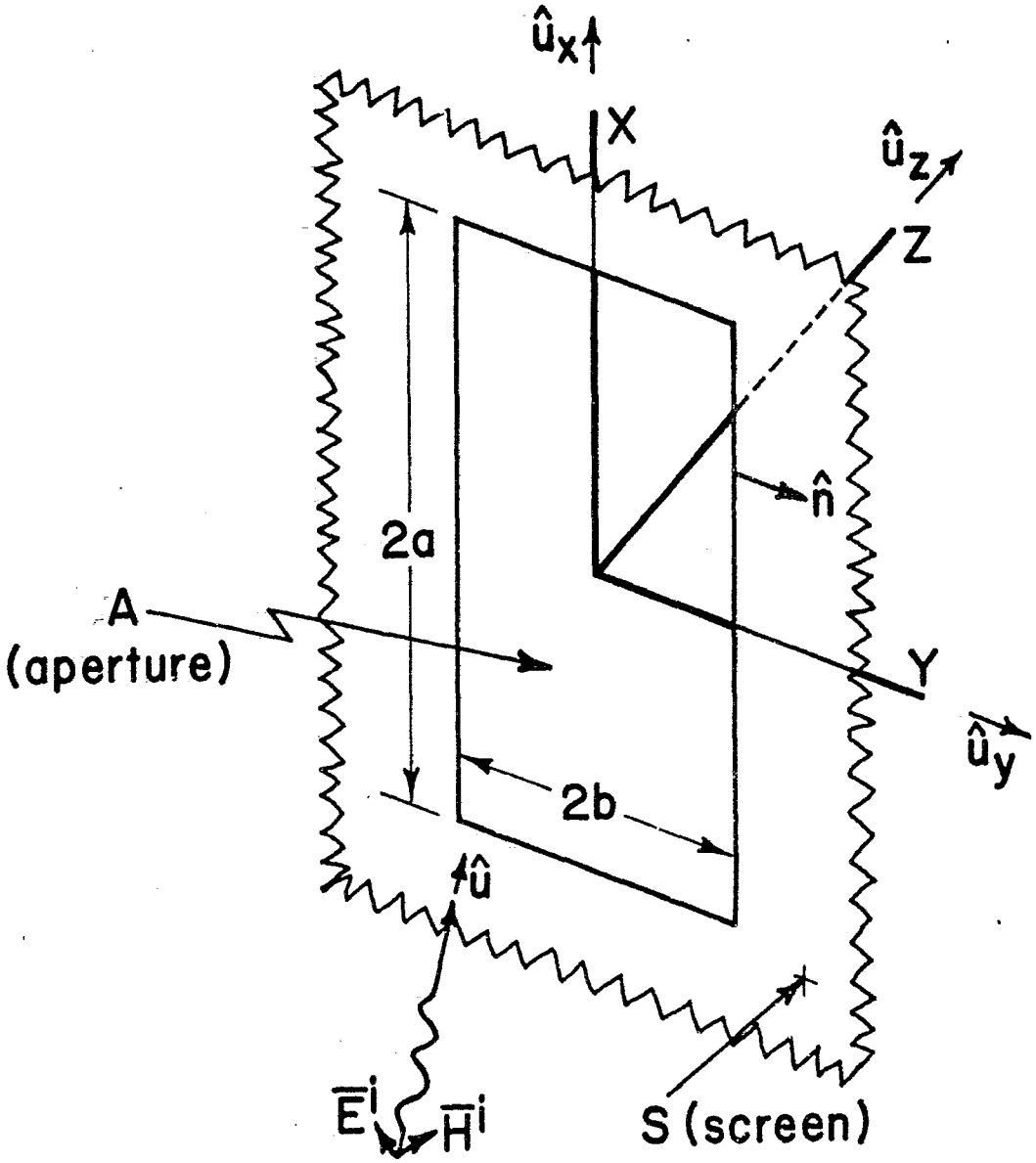

Figure 5. Rectangular Aperture in Conducting Screen

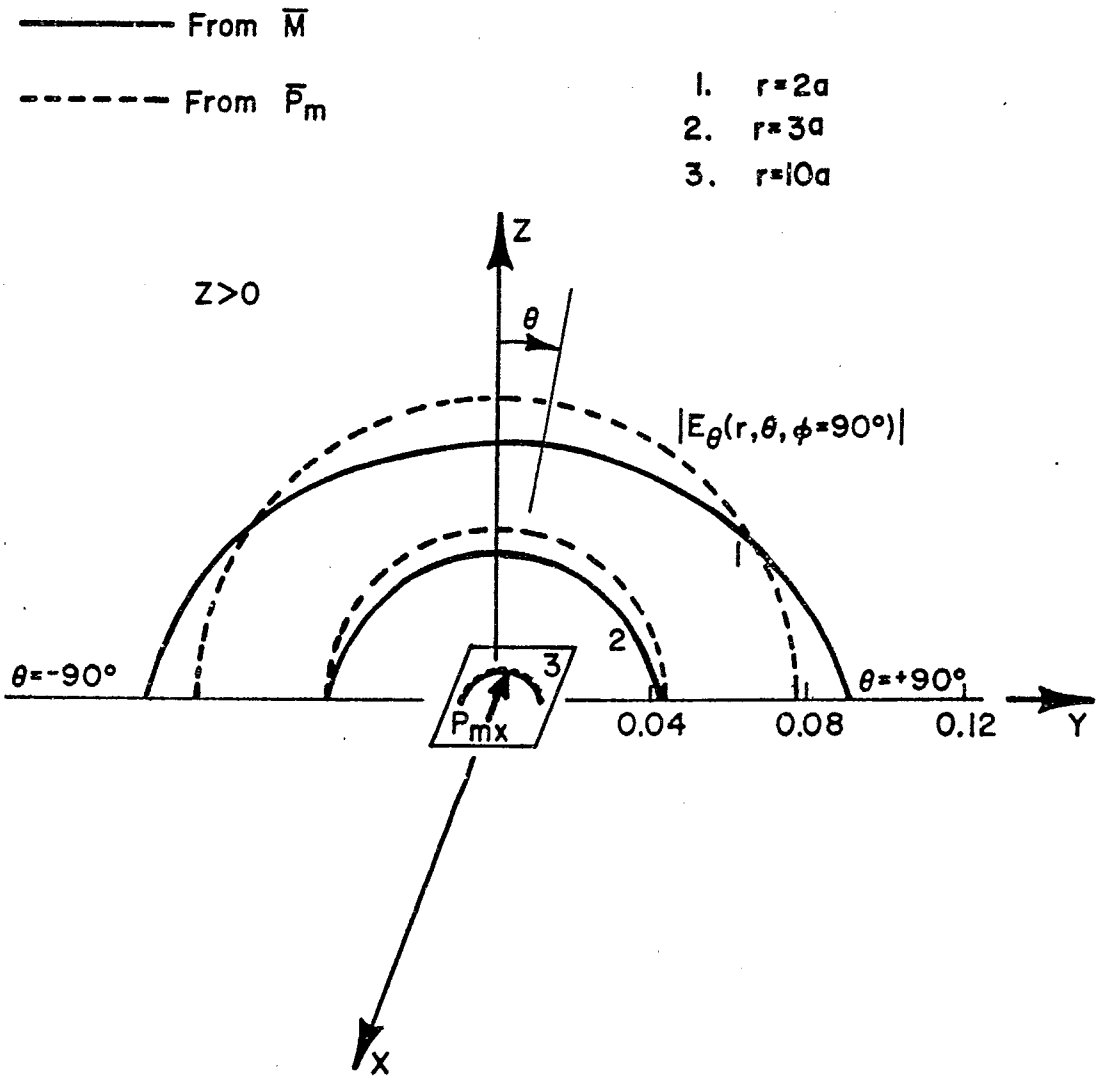

Figure 6. Electric Field on Shadow Side of Square Aperture
($2a = 2b = 0.15\lambda$, $\overline{e}^i = 1\ \hat{u}_y$ Volt/Meter, Normal Incidence)

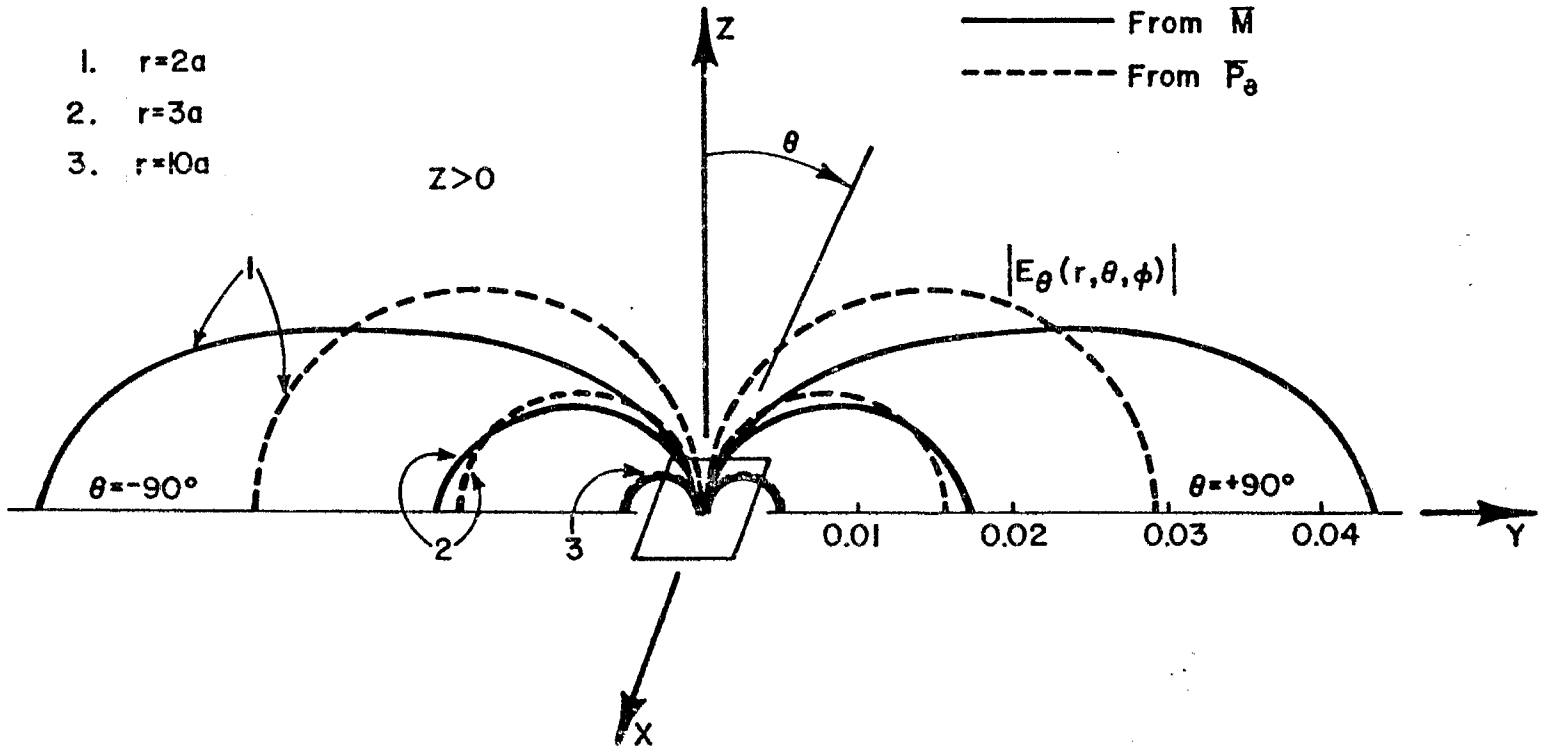

Figure 7. Electric Field on Shadow Side of Square Aperture
($2a = 2b = 0.15\lambda$, $\overline{e}^i = 1\ \hat{u}_z$ Volt/Meter, Edge-On Incidence)

SECTION V

OTHER DATA

Additional data of ancillary interest are presented in Figures 8-14 which depict illuminated-side magnetic current in the presence of the screen subject to various incident fields. The illuminated-side magnetic current in the presence of the screen is related to the total tangential electric field in the aperture by $\overline{E}=\overline{M} \times \hat{u}_z$ (Figure 1).

Figure 8 provides data for an aperture larger than $\frac{\lambda}{2}$ across. Figures 9-11 display partial magnetic currents in small rectangular apertures of different sizes so that one may assess the sensitivity of the magnetic current to increases in a rectangle side length; also for comparison of theories, these figures include results calculated from the Rayleigh series theory (first order) [1] and from the dynamic theory [2].

Figures 12 and 13 give magnetic currents for narrow, rectangular slots of two lengths. The Rayleigh series results (first order) are compared with results obtained from narrow-slot theory [4].

Figure 14 depicts zeroth order magnetic current in a square aperture and values along various cuts parallel to x to y are given.

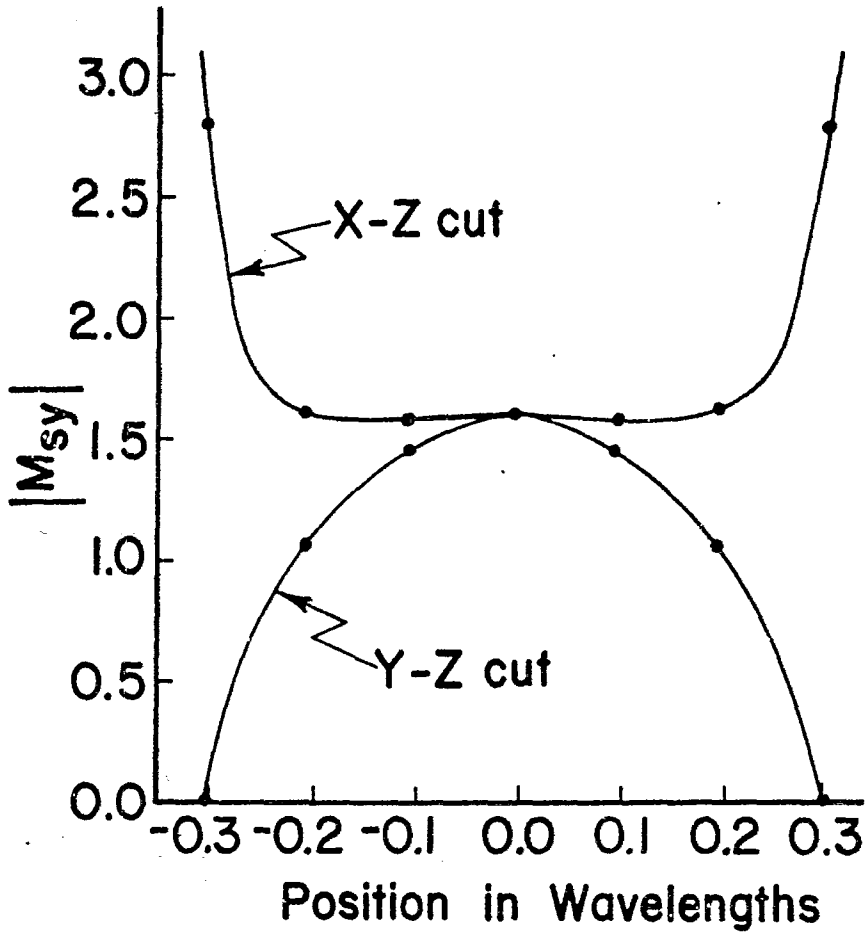

Figure 8. Dynamic Magnetic Current (in Presence of Screen) in a $0.6\lambda \times 0.6\lambda$ Square Aperture ($\vec{e}^{i} = 1\ \hat{u}_x$ Volt/Meter, Normal Incidence)

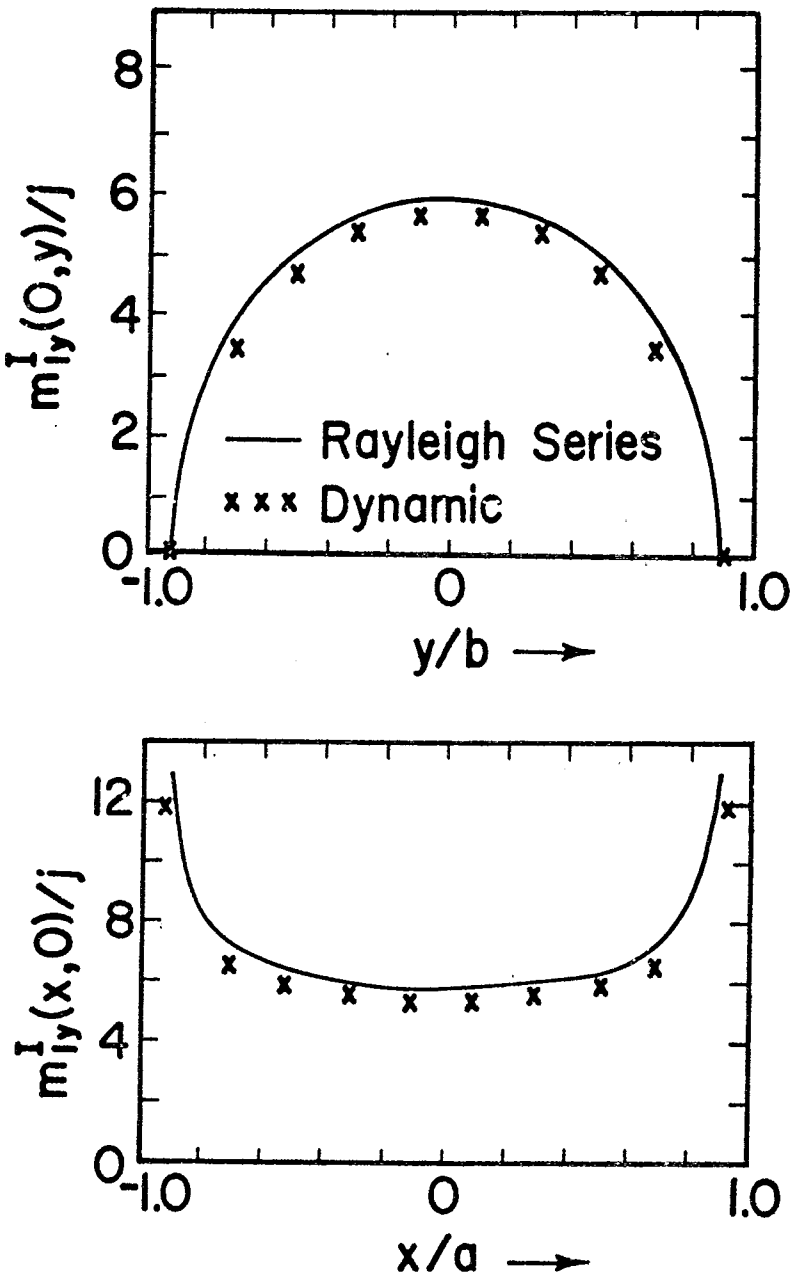

Figure 9. Illuminated-Side Partial Magnetic Current (in Presence of Screen) For Small Square Aperture

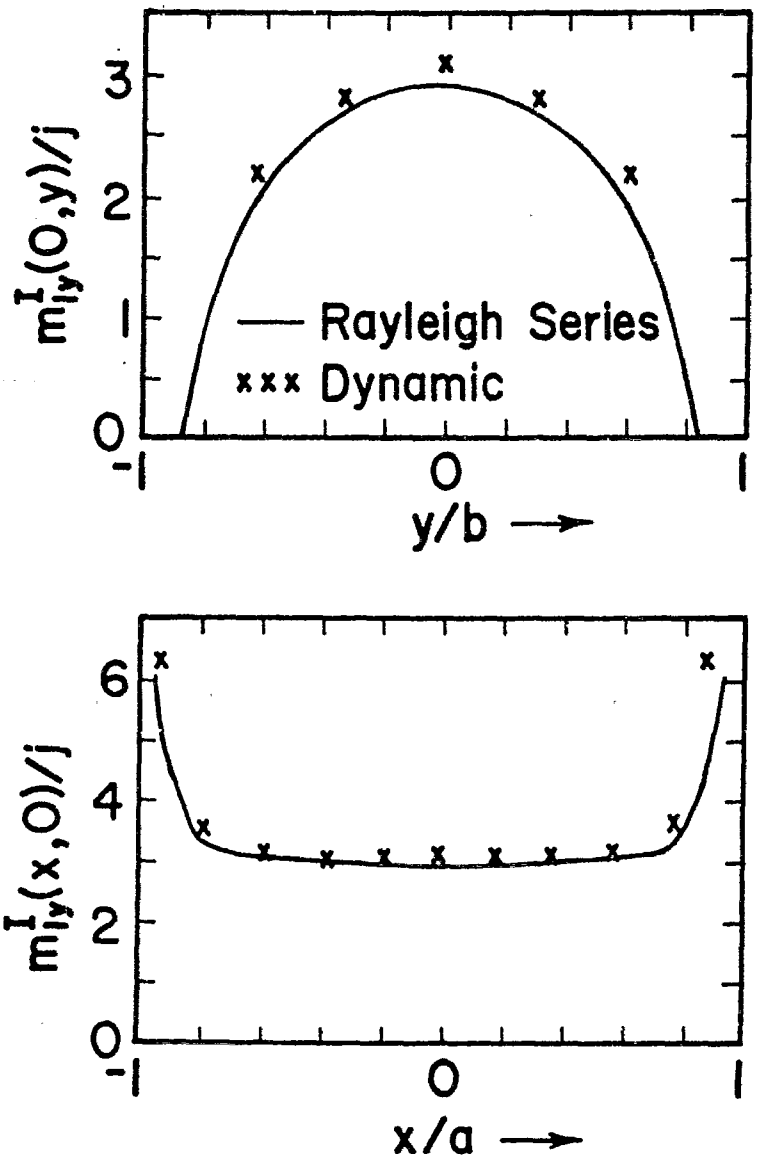

Figure 10. Illuminated-Side, Partial Magnetic Current (in Presence of Screen) For Small Rectangular Aperture (d = a = 2b)

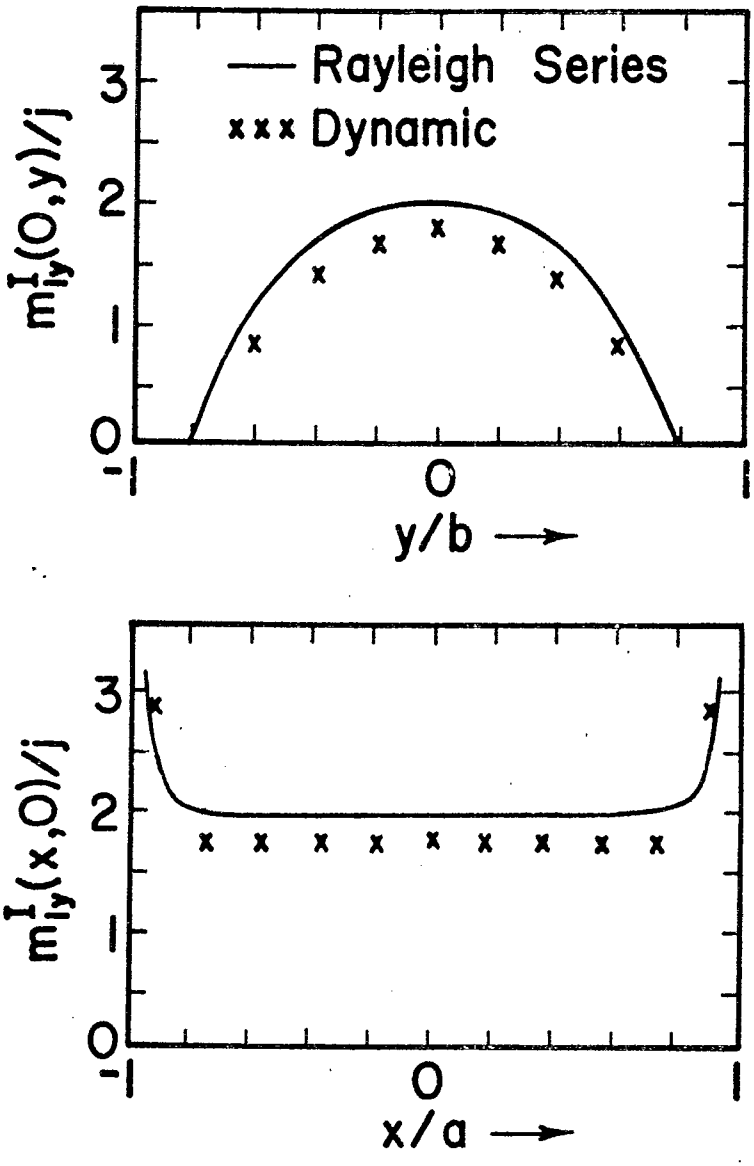

Figure 11. Illuminated-Side, Partial Magnetic Current (in Presence of Screen) For Small Rectangular Aperture (d = a = 3b)

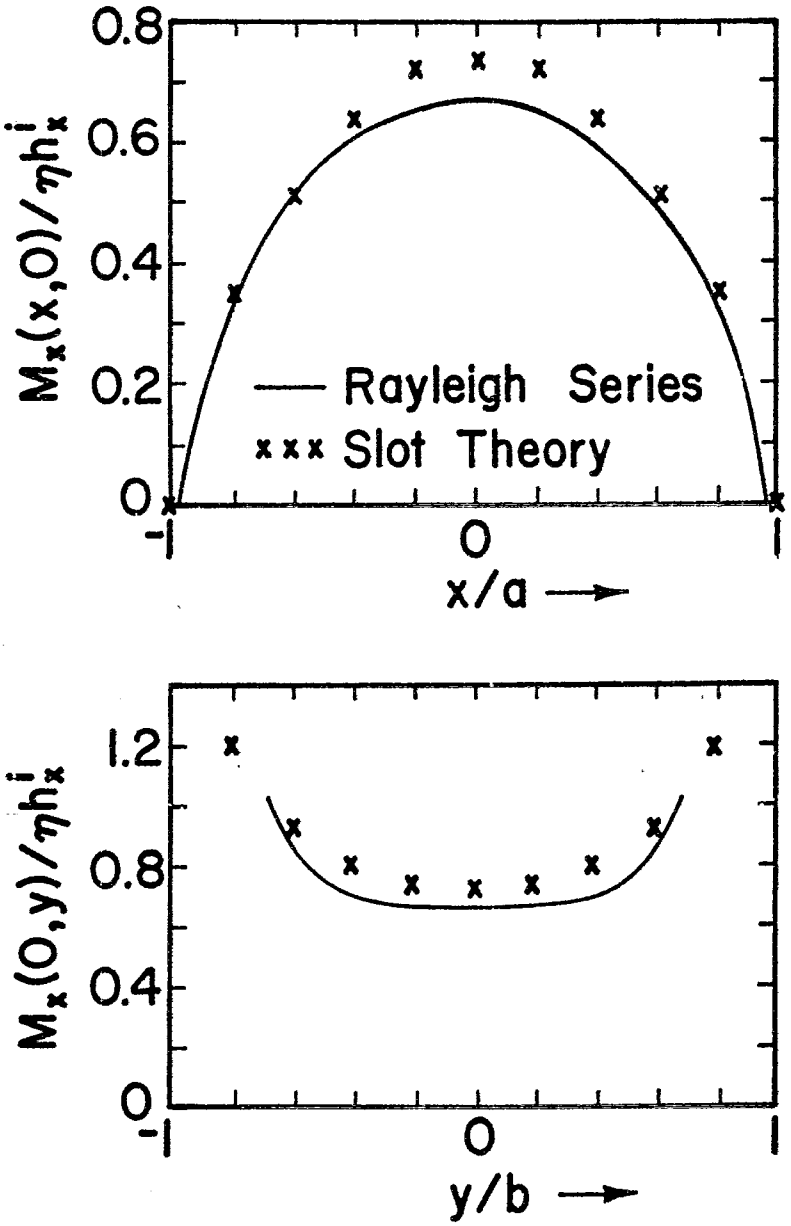

Figure 12. Illuminated-Side, Axial Magnetic Current (in Presence of Screen) in Narrow Rectangular Aperture ($2a = 0.1\lambda$, $2b = 0.01\lambda$, Normal Incidence)

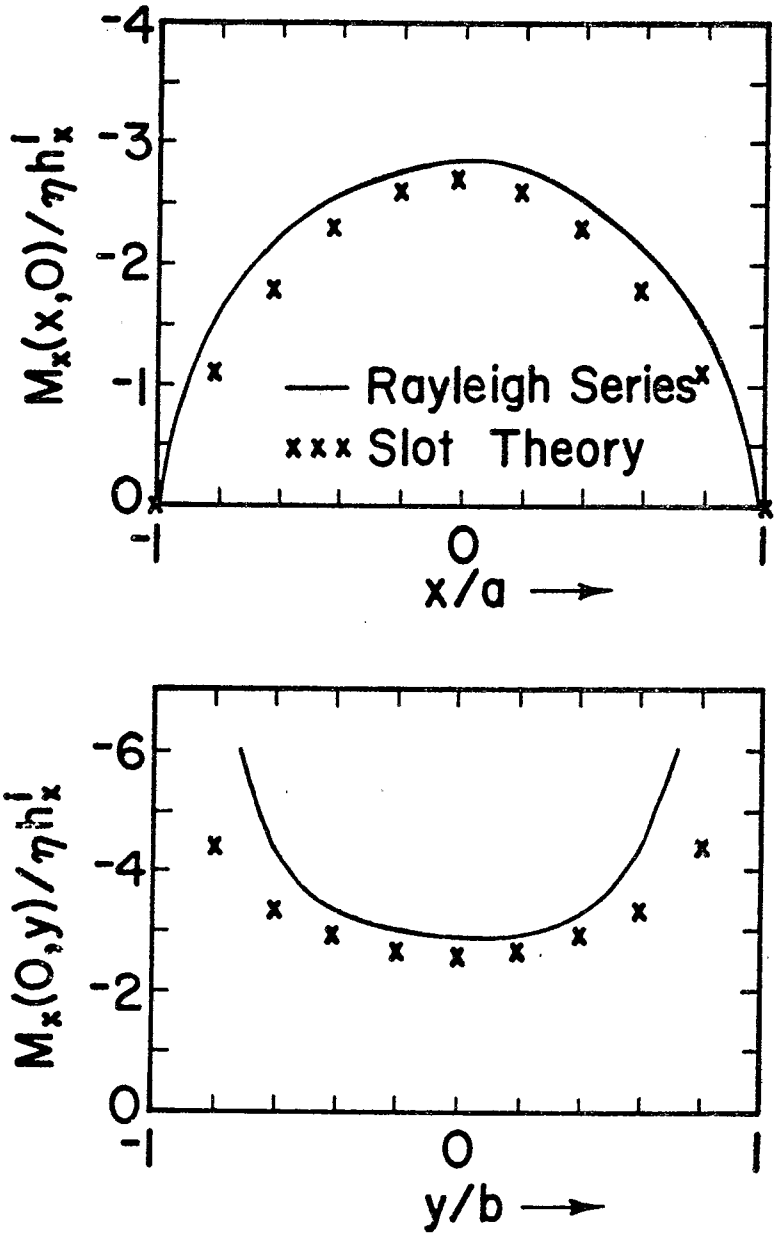

Figure 13. Illuminated-Side, Axial Magnetic Current (in Presence of Screen) in Narrow Rectangular Aperture ($2a = 0.2\lambda$, $2b = 0.01\lambda$, Normal Incidence)

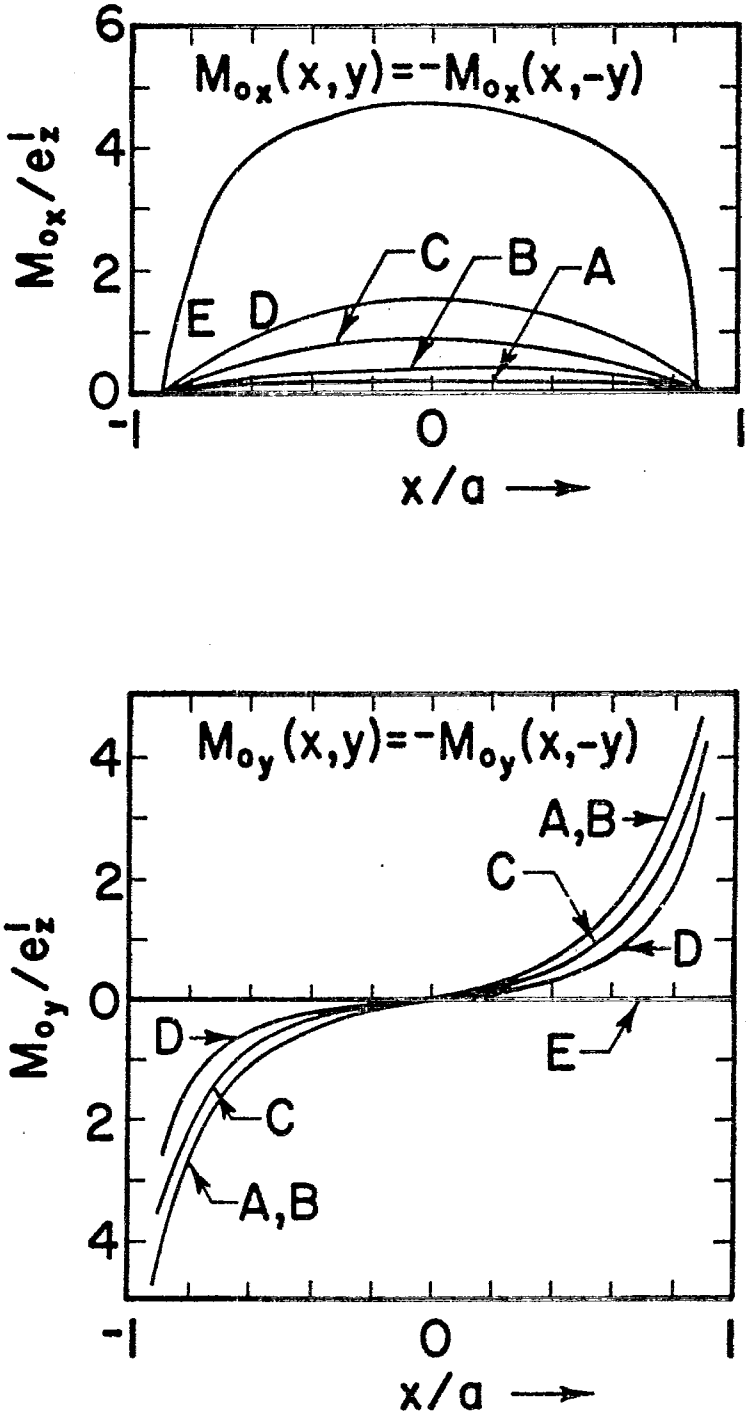

Case	y/b
A	-0.1
B	-0.3
C	-0.5
D	-0.7
E	-0.9

Figure 14. Zeroth Order, Illuminated-Side Magnetic Current in Square Aperture (in Presence of Screen): X Variation along Cuts Parallel to X-Z Plane

REFERENCES

1. Butler, C.M., "Formulation of Integral Equations for an Electrically Small Aperture in a Conducting Screen," Interaction Note 149, Dec. 1973.
2. Wilton, D.R., and O.C. Dunaway, "Electromagnetic Penetration Through Apertures of Arbitrary Shape: Formulation and Numerical Solution Procedure," Interaction Note 214, July 1974.
3. Umashankar, K.R., and C.M. Butler, "A Numerical Solution Procedure for Small Aperture Integral Equations," Interaction Note 212, July 1974.
4. Butler, C.M., "Analysis of a Wire Excited through an Aperture-Perforated Conducting Screen," 1974 USNC/URSI-IEEE Meeting, Boulder, Colo.; Oct., 1974.